Coherence-Incoherence Crossover and the Mass-Renormalization Puzzles in Sr_{2}RuO_{4}

Jernej Mravlje, Markus Aichhorn, Takashi Miyake, Kristjan Haule, Gabriel Kotliar, and Antoine Georges

Phys. Rev. Lett. **106**, 096401 — Published 2 March 2011

DOI: 10.1103/PhysRevLett.106.096401

The coherence-incoherence crossover and the mass-renormalization puzzles in Sr_2RuO_4

Jernej Mravlje,[1,2] Markus Aichhorn,[3,1] Takashi Miyake,[4,5]
Kristjan Haule,[6] Gabriel Kotliar,[6] and Antoine Georges[1,7,5]

[1] *Centre de Physique Théorique, École Polytechnique, CNRS, 91128 Palaiseau Cedex, France*
[2] *Jožef Stefan Institute, Jamova 39, Ljubljana, Slovenia*
[3] *Institute of Theoretical and Computational Physics, TU Graz, Petersgasse 16, Graz, Austria*
[4] *Nanosystem Research Institute, AIST, Tsukuba 305-8568, Japan*
[5] *Japan Science and Technology Agency, CREST, Kawaguchi 332-0012, Japan*
[6] *Physics Department and Center for Materials Theory, Rutgers University, Piscataway NJ 08854, USA*
[7] *Collège de France, 11 place Marcelin Berthelot, 75005 Paris, France*

We calculate the electronic structure of Sr_2RuO_4, treating correlations within dynamical mean-field theory. The approach successfully reproduces several experimental results and explains the key properties of this material: the anisotropic mass renormalization of quasiparticles and the crossover into an incoherent regime above a low temperature scale. While the orbital differentiation originates from the proximity of the van Hove singularity, strong correlations are caused by the Hund's coupling. The generality of this mechanism for other correlated materials is pointed out.

PACS numbers: 71.27.+a,72.15.Qm,75.20.Hr

Fermi-liquid theory describes the low-energy excitations of metals in terms of quasiparticles, which carry the quantum numbers of a bare electron but have a renormalized mass m^*. Quasiparticles have infinite lifetime on the Fermi surface and at temperature $T = 0$, but otherwise acquire a finite lifetime $\hbar/\Gamma$. They carry only a fraction Z of the total spectral weight associated with all single-particle excitations, as encoded in the spectral function $A(\mathbf{k}, \omega)$. A hallmark of strong correlations is that some of these interaction-induced renormalizations (m^*, Z^{-1}, Γ) become large.

The concept of a quasiparticle is meaningful only as long as its inverse lifetime is smaller than the typical excitation or thermal energy $\hbar\Gamma \lesssim \hbar\omega, kT$. The internal consistency of Fermi-liquid theory rests on $\hbar\Gamma \sim (kT)^2/E_F^* \sim (\hbar\omega)^2/E_F^*$, due to phase-space constraints. For temperatures larger than a coherence scale T^* ($\sim E_F^*/k$), quasiparticles become short-lived and the Landau Fermi-liquid description no longer applies. Due to strong correlations, T^* can be much lower than the bare electronic scale E_F/k. The description of the incoherent regime $T > T^*$ and of the associated crossover is a major challenge which requires new concepts and techniques.

Of all transition metal oxides, the layered perovskite Sr_2RuO_4 is undoubtedly the one in which the Fermi liquid regime has been most studied [1]. Resistivities obey accurately a T^2 law for $T \lesssim 30$K [2], despite the large anisotropy $\rho_c/\rho_{ab} \sim 10^3$. Sr_2RuO_4 is also an ideal material to investigate the crossover into the incoherent regime. Indeed, at 130K, $\rho_c(T)$ reaches a maximum and decreases as temperature is further increased, while the T-dependence of ρ_{ab} remains metallic. ARPES studies indicate that quasiparticle peaks disappear (by broadening and loosing spectral weight) at a temperature close to that where ρ_c reaches its maximum [3, 4].

The 3-sheet Fermi surface of this material has been accurately determined by quantum oscillation experiments [1] and is reasonably well described by electronic structure calculations in the local density approximation (LDA) [5]. On the other hand, the measured masses are not reproduced by the LDA. Three bands of mainly t_{2g} character cross the Fermi surface. The broadest (3.5 eV) band of xy character gives rise to a two-dimensional Fermi surface sheet γ. The degenerate xz and yz orbitals give rise to narrower (1.5 eV) bands with quasi one-dimensional Fermi surface sheets α and β. Experimentally, large and *anisotropic* mass enhancements $m^*/m_{\rm LDA}$ are found, namely $(3, 3.5, 5.5)$ for sheets α, β, γ, respectively [1].

These experimental findings raise several puzzles, unresolved to this day. The large effective masses and the low coherence scale indicate that Sr_2RuO_4 is a strongly correlated material. Surprisingly [6], the largest mass enhancement is actually observed for the widest (xy) band. Furthermore, Ru being a $4d$ element, the screened on-site repulsion is not expected to be large ($U \lesssim 3$ eV, somewhat smaller than the bandwidth). In a nutshell, these puzzles can be loosely summarized by the question: why is Sr_2RuO_4 strongly correlated ?

In this letter, we answer these questions in terms of the electronic structure of the material. Treating correlation effects within dynamical mean-field theory (DMFT), we achieve quantitative agreement with experiments. At a qualitative level, our explanation relies on the Hund's coupling J and the proximity of the van Hove singularity for the xy band. These key elements of our picture, especially the Hund's coupling, have general relevance to $4d$ transition-metal oxides, as well as to other materials in which strong correlation effects are observed but are not due to a strong Hubbard U or the proximity to a Mott insulator.

The calculations use the full potential implementation

J [eV]	$m^*/m_{\rm LDA}\|_{xy}$	$m^*/m_{\rm LDA}\|_{xz}$	T^*_{xy}[K]	T^*_{xz}[K]	$T_>$[K]
0.0, 0.1	1.7	1.7	> 1000	> 1000	> 1000
0.2	2.3	2.0	300	800	> 1000
0.3	3.2	2.4	100	300	500
0.4	4.5	3.3	60	150	350

TABLE I. Mass enhancement of the xy and xz orbitals, as a function of Hund's coupling, for $U = 2.3$ eV. Other columns: coherence temperatures as defined in the text.

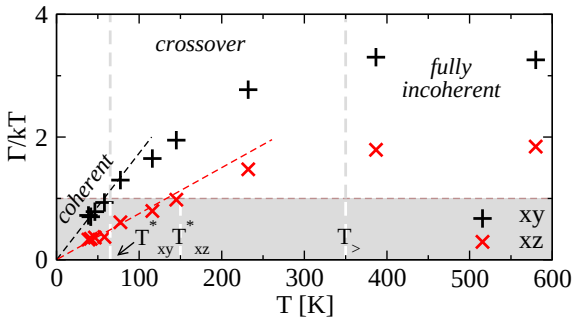

FIG. 1. Temperature-dependence of Γ/kT, with $\hbar/\Gamma$ the quasiparticle lifetime. The shading indicates the 'coherent' regime with long-lived quasiparticles such that $\Gamma \lesssim kT$.

of LDA+DMFT as presented in Ref. [7]. The framework of Ref. [8] gives very similar results. Wannier-like t_{2g} orbitals are constructed out of Kohn-Sham bands within the energy window $[-3, 1]$ eV with respect to the Fermi energy. We use the full rotationally invariant interaction appropriate for a correct description of atomic multiplets:

$$H_I = U \sum_m n_{m\uparrow} n_{m\downarrow} + \sum_{m<n,\sigma} [U' n_{m\sigma} n_{n\bar{\sigma}} + (U' - J) n_{m\sigma} n_{n\sigma} - J c^\dagger_{m\sigma} c_{m\bar{\sigma}} c^\dagger_{n\bar{\sigma}} c_{n\sigma}] - J \sum_{m<n} [c^\dagger_{m\uparrow} c^\dagger_{m\downarrow} c_{n\uparrow} c_{n\downarrow} + h.c.] \quad (1)$$

where J is the Hund's coupling constant, $U' = U - 2J$ and m, n run over t_{2g} orbitals. Ru e_g and O p orbitals are not explicitly included. The importance of correlations leading to charge transfer among the orbitals, mass renormalizations and satellites was recognized in earlier studies [9]. We use the strong-coupling continuous-time Monte-Carlo impurity solver [10] in order to reach the low-temperature regime where the coherence-incoherence crossover takes place [11]. We calculated the interaction parameter U from first-principles using constrained-RPA [12]. The interaction matrix is found to be quite isotropic with $U = 2.5$ eV for xy and $U = 2.2$ eV for xz orbitals. The stronger mass enhancement of the xy orbital can thus not be explained by an anisotropy of the interactions [6].

We now turn to results. In table I we report the mass enhancements of each orbital, given within DMFT by: $m^*/m_{\rm LDA} = Z^{-1}\big|_{T\to 0}$ with $Z^{-1} = 1 - \partial {\rm Im}\Sigma(i\omega)/\partial\omega\big|_{\omega\to 0^+}$. The derivative is extracted by fitting a fourth-order polynomial to the data for the lowest six Matsubara frequencies. The calculated mass enhancements for $U = 2.3$ eV, $J = 0.4$ eV (used in the remainder of the paper [13]) are found to be close to the experiment [1].

Table I demonstrates that the Hund's coupling is essential to reproduce the observed magnitude of mass enhancements and the $xy - xz$ differentiation. A comparable mass enhancement (but without $xy - xz$ differentiation) occurs at $J = 0$ only for the unphysically large $U = 5$ eV. In addition we find that, by favoring maximal angular momentum, the Hund's coupling drives the populations of orbitals closer to one another (to 1.29 and 1.36, for xy and xz, respectively) in comparison to the LDA value $(1.23, 1.39)$, hence improving the agreement with quantum oscillations experiments ($\sim 1.33, 1.33$).

To understand the coherence-incoherence crossover, we display in Fig. 1 the inverse quasiparticle lifetime, plotted as Γ/kT *vs.* T, with $\Gamma = -Z{\rm Im}\Sigma({\rm i}0^+)$. At very low temperatures the Fermi-liquid $\Gamma \propto T^2$ behavior is indicated (dashed). We define the coherence scale T^* by $\Gamma(T^*)/kT^* = 1$, but the deviations from T^2-law are visible already at lower temperatures. T^* is reported in Table I and also indicated on Fig. 1. We see that T^* is as low as 60 K for the most correlated xy orbital. At high temperatures $T \gtrsim T_> \sim 400$ K, Γ/kT saturates, signaling the 'incoherent' regime characterized by a quasi-linear temperature dependence $\Gamma \propto kT$. An intermediate crossover region where Γ/kT gradually increases connects these two regimes.

How do these regimes reveal themselves when probed by spectroscopic experiments? The left-most panel of Fig. 2 displays an intensity map of the momentum-resolved spectral function demonstrating that our results compare well with ARPES [14]. Panels (b) and (c) display the energy-distribution curves at two specific momenta. In the 'coherent' regime, these spectra display sharp peaks corresponding to the Fermi surface crossings. Upon increasing temperature the quasiparticle peaks broaden and above $T_>$ cannot be discerned anymore. Note that in ARPES [3] the peaks disappear already at a somewhat lower temperature, possibly due to the finite momentum resolution in experiment.

The crossover scale $kT_>$ manifests itself also in the dependence of the self-energy on frequency, displayed in the rightmost panels of Fig. 2. We observe that deviations from the low-frequency Fermi liquid regime ${\rm Re}\Sigma \sim \Sigma(0) + \omega(1 - 1/Z)$, ${\rm Im}\Sigma \sim \omega^2 + (\pi T)^2$ appear at an energy scale of order 40 meV$\sim kT_>$, at which a 'kink' [16] is observed in ${\rm Re}\Sigma(\omega)$. Such a feature at that energy scale is indeed reported in ARPES (Fig. 2) [15, 17].

The crossover also affects the magnetic response. On Fig. 3(a) we display the orbitally resolved uni-

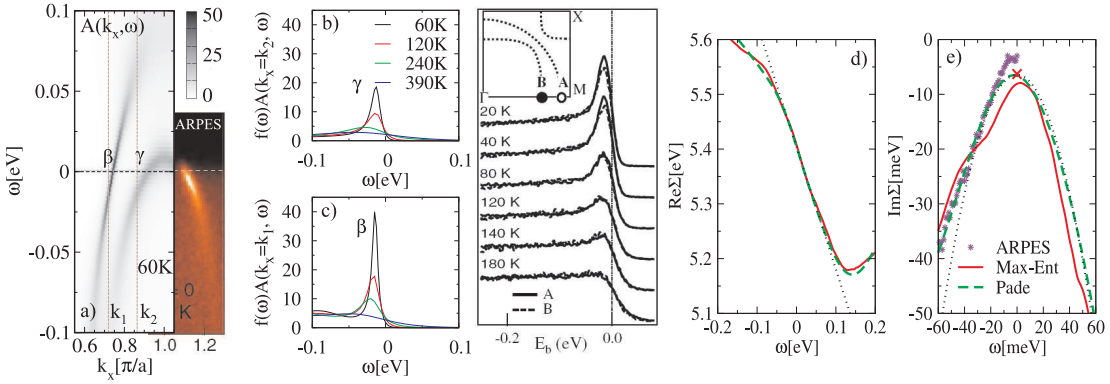

FIG. 2. (a) Intensity map of the spectral function $A(k,\omega)$ along $\Gamma \rightarrow$M for $0.55\pi/a \leq k_x \leq 1.05\pi/a$, $k_y = 0$ at $T = 60$ K compared to ARPES [14]. (b,c) Spectral lineshapes at wavevectors k_1, k_2 compared to ARPES [3]. (d,e) $\mathrm{Im}\Sigma(\omega + \mathrm{i}0^+)$ and $\mathrm{Re}\Sigma(\omega + \mathrm{i}0^+)$ for xz orbital at $T = 60$ K obtained by stochastic maximum entropy (plain line) and Pade approximants (dashed) compared to ARPES [15]. Also indicated (cross,dotted line) are the low-ω behavior from a polynomial fit.

form magnetic susceptibilities and compare them to the NMR Knight shift measurements [18]. Saturation to a Pauli magnetic susceptibility is observed only below T^* (shaded). The stronger temperature dependence of the xy orbital related to $T^*_{xy} < T^*_{xz}$ is reproduced well. The total low temperature uniform susceptibility (1.2 emu/mol) is within the estimated error ($\sim$ 30% [18]) of the thermodynamic measurements (0.9 emu/mol) [19]) [20]. We also calculated the local susceptibility (inset) and found that it is larger than the uniform one, especially for the xz orbital [21]. This signals *antiferromagnetic* correlations, in agreement with experimental observations [22].

In Fig. 3(b) we display $\lim_{\omega\to 0}\sum_q \mathrm{Im}\chi(q,\omega)/\omega$ and compare to the NMR data for $1/T_1T$ (we used the values of hyperfine couplings from Refs. [22, 23]). There, the data saturate only well below T^*, illustrating that the Fermi liquid behavior in two-particle properties is more fragile than in single-particle ones. Indeed, in the well known Kondo problem the Kondo resonance persists at temperatures up to $2T_K$ while the magnetic susceptibility saturates to a Pauli form only below $T_K/5$.

Having demonstrated that the LDA+DMFT results agree with experimental data, we turn to theoretical insights. In DMFT the local physics is revealed by solving an impurity model (atom + bath) with atomic interactions given by Eq. (1). This can be rewritten as $H_I = (U-3J)n(n-1)/2 - 2JS^2 - (J/2)T^2$, where S is the total spin and T is the total angular momentum [24]. The four-electrons subspace separates into five $T = 2, S = 0$ states, a single $T = 0, S = 0$ state and nine $T = 1, S = 1$ states. At $J = 0$ all these states are degenerate and form a 15-dimensional representation of an $SU(6)$ symmetry group. This high degeneracy results in a very high coherence scale $\sim$ 0.5eV and small mass renormalizations (see Table I). The Hund's coupling J lowers

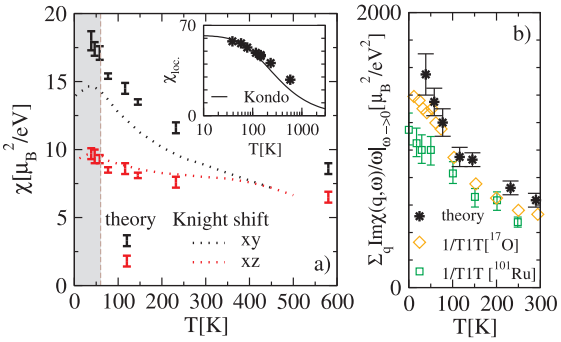

FIG. 3. (a) The uniform susceptibility $\chi_m(q=0)$ for each orbital, $m = xy, xz$. (Inset) Total local susceptibility $\chi_{\mathrm{loc.}} = \sum_{qm}\chi_m(q)$ compared to that of the S=1 Kondo model. (b) $\lim_{\omega\to 0}\sum_q \mathrm{Im}\chi(q,w)/\omega$ compared to NMR [18].

the SU(6) symmetry down to $\mathrm{SU(2)_{spin}} \times \mathrm{SU(2)_{orbit}}$ with the 9-fold degenerate atomic multiplet $S = 1, T = 1$ having lowest energy. The ground state of the impurity model is non-degenerate with $S = 0, T = 0$ corresponding to exact screening of this atomic multiplet [24]. Thus Sr_2RuO_4 is a Fermi liquid. The Hund's coupling projects the spin degrees of freedom onto a low-energy manifold characterized by a reduced Kondo coupling, resulting in a suppressed Kondo scale [25, 26]. The effective low energy model is in our case a $S = 1$ Kondo model. Indeed, the inset of Fig. 3(a) demonstrates that at low T the LDA+DMFT result for $\chi_{\mathrm{loc.}}$ is fit well by the $S = 1$ Kondo model Bethe ansatz curve [27]. The dramatic reduction of coherence scale as a result of the Hund's coupling has been noted before in impurity models [25, 26, 28], DMFT studies of model Hamiltonians [29] and for iron pnictides [30]. It occurs whenever multiplet correlations persist while the on-site U is strongly

screened (due to the large spatial extension of the correlated orbital as in $4d$ transition metal oxides, or the large polarizability of screening orbitals as in pnictides).

The origin of the larger xy effective mass can be traced to the proximity of the van-Hove singularity. Higher density of states near the Fermi level implies weaker dispersion and in turn reflects in a lower value of the respective hybridization function $\Delta(i\omega)$ at low frequencies (Fig. 4). Indeed, ignoring the self-consistency (i.e. on the first DMFT iteration), $\mathrm{Im}\Delta^{(1)}(i0^+) = -\pi\rho_F/\left[\mathrm{Re}G_{\mathrm{loc}}(i0^+)^2 + (\pi\rho_F)^2\right] \simeq -1/(\pi\rho_F)$ with ρ_F the LDA density of states at the Fermi level. The large value of ρ_F thus corresponds to a suppressed low-energy effective hopping [31]. In contrast, the full bandwidth is larger for the xy, and so is the LDA kinetic energy (0.27eV for xy, 0.20eV for xz). This reflects in the high-frequency behavior of the hybridization, indeed larger for xy at high-frequency. Note that the degree of correlation cannot be guessed from the kinetic energy or bandwidth of each band, which would naively suggest a smaller mass for xy, in contrast to observations.

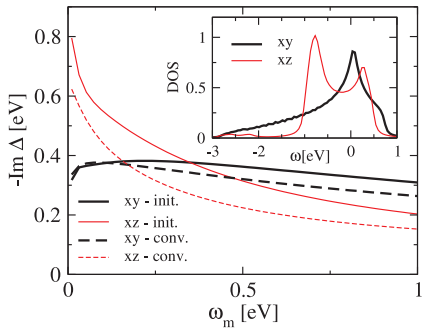

FIG. 4. The hybridization functions $\Delta(i\omega)$ at the initial DMFT step and at self consistency. (Inset) The LDA projected density of states.

In summary, we have demonstrated that several experimental results for Sr_2RuO_4 are well reproduced by the LDA+DMFT method. We have shown that the suppression of the coherence scale is due to the Hund's coupling, and pointed out the generality of this mechanism. We have also shown that the orbital differentiation and larger xy mass is due to the difference in low-energy hybridization properties of each orbital, caused by their orientation-dependent bonding properties in this anisotropic material. This is expected to be relevant to other layered perovskites, most notably to the metal-insulator transition in $Ca_{2-x}Sr_xRuO_4$.

We are grateful to P. Bourges, M. Fabrizio, M. Ferrero, E. Gull, L. de Leo, A. Mackenzie, Y. Sidis and M. Sigrist for useful discussions. We acknowledge the support of the NSF-materials world network (NSF DMR 0806937), the Partner University Fund, the CNRS-LIA program, the Austrian Science Fund (projects J2760, F4103, P18551) and the hospitality of KITP, Santa Barbara (NSF PHY05-51164) and of CPHT (G.K.).

[1] A. P. Mackenzie and Y. Maeno, Rev. Mod. Phys. **75**, 657 (2003); C. Bergemann *et al.*, Adv. Phys. **52**, 639 (2003).
[2] N. E. Hussey *et al.*, Phys. Rev. B **57**, 5505 (1998).
[3] S.-C. Wang *et al.*, Phys. Rev. Lett. **92**, 137002 (2004).
[4] T. E. Kidd *et al.*, Phys. Rev. Lett. **94**, 107003 (2005); see also T. Valla *et al.*, Nature **417**, 627 (2002).
[5] T. Oguchi, Phys. Rev. B **51**, 1385 (1995); D. J. Singh, *ibid.* **52**, 1358 (1995).
[6] R. M. Konik and T. M. Rice, Phys. Rev. B **76**, 104501 (2007).
[7] M. Aichhorn *et al.*, Phys. Rev. B **80**, 085101 (2009).
[8] K. Haule *et al.*, Phys. Rev. B **81**, 195107 (2010).
[9] A. Liebsch and A. Lichtenstein, Phys. Rev. Lett. **84**, 1591 (2000); V. Anisimov *et al.*, Eur. Phys. J. B **25**, 191 (2002); Z. V. Pchelkina *et al.*, Phys. Rev. B **75**, 035122 (2007); see also E. Gorelov, M. Karolak, T. O. Wehling, F. Lechermann, A. I. Lichtenstein, and E. Pavarini, Phys. Rev. Lett. **104**, 226401 (2010).
[10] P. Werner *et al.*, Phys. Rev. Lett. **97**, 076405 (2006); see also K. Haule, Phys. Rev. B **75**, 155113 (2007).
[11] We use $> 10^7$ Monte Carlo steps per iteration and 10^6 steps for the thermalization. Worst average sign > 0.997.
[12] F. Aryasetiawan *et al.*, Phys. Rev. B **70**, 195104 (2004); For technical details see T. Miyake and F. Aryasetiawan, *ibid.* **77**, 085122 (2008).
[13] Extracting J from the reduced $J_{mm'}$ matrix calculated by constrained RPA yielded $J = 0.25$eV, although a somewhat larger value is expected to be obtained when considering the full $U_{m_1m_2m_3m_4}$ matrix.
[14] K. M. Shen *et al.*, Phys. Rev. Lett. **99**, 187001 (2007).
[15] N. J. C. Ingle *et al.*, Phys. Rev. B **72**, 205114 (2005).
[16] K. Byczuk *et al.*, Nat. Phys. **3**, 168 (2007).
[17] Y. Aiura *et al.*, Phys. Rev. Lett. **93**, 117005 (2004).
[18] T. Imai *et al.*, Phys. Rev. Lett. **81**, 3006 (1998).
[19] Y. Maeno *et al.*, J. Phys. Soc. Jpn **66**, 1405 (1997).
[20] The NMR estimates (dots) are thus multiplied by 1.3, to ease the comparison of the temperature dependence.
[21] $\chi_m(q=0)^{-1} - [\sum_q \chi_m(q)]^{-1}$, averaged over the temperature interval, are $0.06, 0.2$ eV$/(g\mu_b)^2$, for xy, xz, resp.
[22] Y. Sidis *et al.*, Phys. Rev. Lett. **83**, 3320 (1999).
[23] K. Ishida *et al.*, Phys. Rev. B **64**, 100501 (2001).
[24] L. de Leo, Ph.D. thesis, SISSA (2004).
[25] I. Okada and K. Yosida, Prog. Theor. Phys. **49**, 1483 (1973).
[26] A. H. Nevidomskyy and P. Coleman, Phys. Rev. Lett. **103**, 147205 (2009).
[27] A single fit parameter $T_K = 240$K in the notation of H.-U. Desgranges, J. Phys. C **18**, 5481 (1985).
[28] T. Pruschke and R. Bulla, Eur. Phys. J. B.
[29] P. Werner, E. Gull, and A. J. Millis, Phys. Rev. B **79**, 115119 (2009).
[30] K. Haule and G. Kotliar, New J. Phys. **11**, 025021 (2009); see also M. Aichhorn *et al.*, Phys. Rev. B **82**, 064504 (2010).
[31] A single band calculation with the orbitally projected density of states at filling 4/3 gives $m^*/m \sim 2.2(1.8)$ and $T^* = 0.05(0.1)$eV for xy (xz). See also R. Žitko,

J. Bonča, and T. Pruschke, Phys. Rev. B **80**, 245112 (2009); S. Schmitt, *ibid.* **82**, 155126 (2010).